Swarm Filtering Procedure
and Application to MRI Mammography

Horia Mihail H. Teodorescu and David J. Malan

Abstract—Research on swarming has primarily focused on applying swarming behavior with physics-derived or ad-hoc models to tasks requiring collective intelligence in robotics and optimization. In contrast, applications in signal processing are still lacking. The purpose of this paper is to investigate the use of biologically-inspired swarm methods for signal filtering. The signal, in the case of images the grayscale value of the pixels along a line in the image, is modeled by the trajectory of an agent playing the role of the prey for a swarm of hunting agents. The swarm hunting the prey is the system performing the signal processing. The movement of the center of mass of the swarm represents the filtered signal. The position of the center of mass of the swarm during the virtual hunt is reverted into grayscale values and represents the output signal. We show results of applying the swarm-based signal processing method to MRI mammographies.

Index Terms—Swarm intelligence, nonlinear signal filter, MRI, mammography, image processing.

I. INTRODUCTION

S WARMING behavior is widely encountered in populations in nature, where the collective intelligence of the swarm has the advantage of better performing tasks such as escaping from predators, exploring terrain in quest of nutrients, or hunting. Swarming is the collective, aggregated, corroborated behavior of a set of individuals (agents) of similar or identical structure, each of them able to sense, move, and make decisions of their own while communicating with the other agents or while observing the other agents' movements. A swarm is said to possess a collective (distributed) intelligence because a specific behavior occurs at the group level. While each agent potentially has full autonomy and decision-making capability, their individual behaviors are aggregated through the coupling of the movements of neighbor agents. This new behavior results from the aggregation of individual movements. Consequently, the displacement of an individual is largely decided at the group level, allowing a swarm to accomplish tasks that would be unreachable to a single agent, or to better accomplish such tasks. Artificial swarms mimic the behavior of groups of insects, fish schools, or herds of animals.

The purpose of this paper is to introduce and demonstrate a novel method of nonlinear filtering based on swarm dynamic. We apply the method to MRI images with the goal of testing

the capabilities of swarm processing. The method we propose transforms an image into a surrounding relief that directly modifies the swarming behavior during hunting. The swarm views the image as a 'ground surface' it flies over. Each agent in the swarm sees the closest pixels as constraints of the movement. We model the signal (process) to be filtered by the dynamic (trajectory) of an agent playing the role of prey. A swarm comprising several hunting individuals hunts a prey, according to a modified swarm procedure. Thus, when the prey follows a line in the image, the swarm averaged trajectory processes a line of the image, filtering the image line and re-morphing it. The resulted filters will be generically named swarm filters. The number of individuals in the swarm and various parameters of the swarm constitute the parameters of the filter. The output (filtered) signals are obtained as the average accelerations of the swarm in the x, y, and z directions of motion. The model we adopted is motivated by the need to create a direct interaction between the swarm and the image, still preserving the main concepts in the swarming theory and a reasonable resemblance with the natural swarming processes. Our hypothesis, which is verified by the preliminary results, was that the swarm 'smoothes', that is, filters and morphs the relief underneath it. At this stage, we manually optimized the type of interactions between the agents and the image 'relief'.

The swarm signal processing pertains to the larger class of nonlinear methods. The nonlinearity of the swarming is produced by the nonlinear terms in the swarm movement equations we use, in the first place the distance-dependent terms, as presented in Section 2. The swarm processing has a different mechanism of operation than other nonlinear signal processing systems, such as neural networks, statistical filters, and dynamic range compression filters. The swarm processing can be thought of as a nonlinear procedure based on a set of nonlinear, second order coupled equations, each describing the movement of an element of the swarm under the constraints imposed by the signal impersonated by the prey.

The swarm model we propose for signal processing combines features from several swarm models presented in the literature and uses a few new constraints and characteristics. Subsequently, we briefly recall several models on which ours relies. Physics-derived models, as described by Elkaim *et al.* [1], often focus on determining discrete models for the positions and speeds of the particles, given close-contact forces between swarm agents, such as spring-type forces in the models of Elkaim [1], [2], and a stronger force to a leader. Olshevsky *et al.* [3], and Olfati-Saber and Murray [4] describe

another set of models involving node-to-node interactions on a graph network. A consensus in the literature is that a constraint in swarm-type applications is communication bandwidth; as a consequence, swarm agents have some form of very elementary memory. Olfati-Saber and Murray [4], [5] propose Markov type I and II models. In many previous models, the accelerations of the swarm agents can have large discontinuities. Some swarm models, illustrated by Elkaim's models in particular allows the swarm the possibility of easily splitting into subgroups after avoiding an obstacle. The use of the center of mass as a virtual leader, as well as the use of the same type of spring force for interactions member-member and member-obstacle contributes to this behavior. We included in our proposed discrete models limits for the allowed accelerations. Also, we use an equation for acceleration that favors more the coherence of the swarm.

Swarming algorithms are strongly dependent on the neighborhood concept and involve the distance between agents. While there is substantial evidence in nature that communication between swarm members is not only through visual interaction, the implicit assumption in the modeling literature is that the distance perception is Euclidean (as in the works of Elkaim *et al.* [2], Murray *et al.* [4]). Anstey *et al.* have shown in a recent Science article [6] that the communication between swarm members that triggers gregarization (or swarming behavior) is done through chemical recognition (smell). Use of communication through odor is also found in populations of wasps [7], of spiders [8], and of bees [9]. Other forms of non-visual communication appear in populations of fish (swarming communication through odor, according to Todd *et al.* [10]) and frogs (evidence of ultrasonic communication is shown in the works of Feng *et al.* [11], and of Arch *et al.* [12]). Therefore, there is no imperative requirement for the usage of Euclidean distance for modeling perception for every application; consequently, we used models based on both Euclidean and non-Euclidean metrics.

Ant colony algorithms are a fundamentally different approach than that of physics-derived swarming models discussed above. Ant colony swarming occurs based on evolution of pheromone fields based on trails left by individual agents, as opposed to neighboring agent interactions. Recently, Ramos *et al.* [13], [14], Huang *et al.* [15], [16], and Ma *et al.* [17] applied ant colony algorithms to image processing for medical images. These authors used the pheromone traces left by the ants to create contour-like images superposed over the initial images. Contour enhancement is not optimal for MRI images due to the gradient variations between areas in the image as opposed to sharper differences between neighboring image areas and an alternate method to ant colony algorithms has to be developed. In our approach, we prefer the swarming, without feromone-like memory, as the model that implements the signal processing.

The organization of the paper is as follows. In the second section we present the details of the proposed swarming model and of its implementation. We present a few image processing results in the third section. The last section comprises conclusions.

II. PROPOSED SWARMING MODEL

We propose a three-dimensional swarm dynamic based on neighbor interactions dependent on nonlinear attraction and repulsion forces. The forces are piece-wise functions dependent on the vicinity criteria. The purpose of the attraction and repulsion forces is to mediate swarm aggregation. Literature models such as those of Elkaim *et al.* [1], [2] propose elastic forces both for attraction and repulsion.

A. General Setting

We say that the vicinity of agent i is dynamic if the neighbors j of i can change over time. The set of neighbors V_i of agent i is recomputed for every timestep. We determine the dynamic vicinity using a fixed-radius model in which the neighbors j of i are determined based on the condition that the distance between the two agents satisfies $d(i, j) \leq \rho$ where we consider ρ to be the radius of a spherical vicinity having agent i at its center. Neighbors who are closer to i than the distance d_{min} are subject to a repulsion force; otherwise neighbors are subject to an attraction force.

While attraction and repulsion forces are responsible for the internal cohesion of the swarm, the swarm is not driven across the input image by the internal forces. An external force is necessary to drive the swarm across the input image. Unlike literature models such as those of Murray *et al.* [4] and Elkaim *et al.* [1] where the purpose of the swarm dynamic is given by a constant bias in the velocity of the swarm agents, our model is a predator-prey model in which the swarm of predator agents is attracted to a prey by an agent-prey force that acts independently on every agent in the swarm. This is a forcing factor in the equations of motion of the swarm. We also consider a friction force that depends on the speed of the agent. Therefore, in the model we propose there are three types of forces that act upon a given swarm agent i: internal swarm attraction/repulsion forces between i and all its neighbors j, external force acting upon agent i from the prey p, and friction forces. The force, $F_x(i)$, acting on agent i in the x direction of motion is the result of:

$$\vec{F}_x(i) = \vec{F}_{friction,x}(i) + \\ + \sum_{j \in V_i} \vec{F}_{internal,x}(i,j) + \vec{F}_{external,x}(i,p) \quad (1)$$

where the notation $j \in V_i$ signifies that we take the contributions from all neighbors j in the vicinity V_i of agent i and the notation (i,j) signifies that the force depends on agents i and j. The general equation above holds also for the y and z directions of motion.

The internal cohesion of the swarm is managed by agent-to-agent attraction and repulsion forces which act

upon neighboring agents. In order to prevent collisions among neighboring agents, a repulsion force acts upon two neighboring agents if the distance between them is less than a threshold $d_{min} < \rho$. An attraction force acts upon neighboring agents otherwise. We chose the following internal cohesion force, where the coefficient of the repulsion force is β and the coefficient of the attraction force is α:

$$\vec{F}_{internal}(i,j) = \begin{cases} \frac{\beta \cdot (\vec{r_i} - \vec{r_j})}{(r_i - r_j)^3} & \text{if } |\vec{r_i} - \vec{r_j}| \le d_{min} \\ \frac{\alpha \cdot (\vec{r_i} - \vec{r_j})}{(r_i - r_j)^4} & \text{if } d_{min} < |\vec{r_i} - \vec{r_j}| \le \rho \end{cases} \quad (2)$$

where $\vec{r_i}$ denotes the position vector of the agent i. The overall swarm cohesion force acting on agent i due to its neighborhood is $\sum_{j \in V_i} \vec{F}_{internal}(i,j)$. Note that the distance function $d(i,j) = |(\vec{r_i} - \vec{r_j})|$ may be chosen as non-Euclidean. In this section we only treat the Euclidean distance case. In subsection 2.5 we briefly discuss a non-Euclidean distance example. The force acting on agent i in the x, y, and respectively z directions due to the neighborhood of i are:

$$\vec{F}_{neighborhood,x}(i,t) = \sum_{j \in V_i} \vec{F}_{internal}(i,j) \cdot$$
$$\cdot \frac{x_i(t-1) - x_j(t-1)}{d(i,j)}$$

$$\vec{F}_{neighborhood,y}(i,t) = \sum_{j \in V_i} \vec{F}_{internal}(i,j) \cdot \quad (3)$$
$$\cdot \frac{y_i(t-1) - y_j(t-1)}{d(i,j)}$$

$$\vec{F}_{neighborhood,z}(i,t) = \sum_{j \in V_i} \vec{F}_{internal}(i,j) \cdot$$
$$\cdot \frac{z_i(t-1) - z_j(t-1)}{d(i,j)}$$

where by the notation (i,t) we refer to the agent i at current moment of time t.

We choose the following velocity-dependent friction force that acts on agent i at time t:

$$\vec{F}_{friction,x}(i,t) = -\mu \cdot \dot{x}_i(t-1)$$

$$\vec{F}_{friction,y}(i,t) = -\mu \cdot \dot{y}_i(t-1) \quad (4)$$

$$\vec{F}_{friction,z}(i,t) = -\mu \cdot \dot{z}_i(t-1)$$

where we consider the friction coefficient μ to be a constant and the same for all agents in the swarm and is in the range $0 \le \mu \le 1$. A higher value of μ implies a faster damping of the movement. Physically the choice of the friction force is appropriate for the motion of the agent in an idealized fluid of low viscosity and with no turbulence.

B. Interaction with the Image

The external force acting on every agent of the swarm is an elastic force that sets the goal for the swarm to follow the trajectory of the prey p. From a physical point of view, this agent-prey force ensures that every agent is attracted to the prey. We choose a prey-agent force of the following expression:

$$\vec{F}_{external,x}(i,p,t) = \lambda_x \cdot (x_p(t-1) - x_i(t-1))$$
$$\vec{F}_{external,y}(i,p,t) = \lambda_y \cdot (y_p(t-1) - y_i(t-1)) \quad (5)$$
$$\vec{F}_{external,z}(i,p,t) = \lambda_z \cdot (z_p(t-1) - z_i(t-1))$$

where $\lambda_x, \lambda_y, \lambda_z$ are coefficients. The use of the prey-agent force in the image processing algorithm is discussed in sect. 2.6.

C. Discretizing the Movement Equations

We will discretize the equations of motion of the swarm agents with a timestep parameter, δ, which we vary in the simulations section. The equations of motion in the x, y, and respectively z direction for agent i are:

$$\{x_i(t) = x_i(t-1) + \delta \cdot \dot{x}_i(t), \ y_i(t) = y_i(t-1) + \delta \cdot \dot{y}_i(t),$$
$$z_i(t) = z_i(t-1) + \delta \cdot \dot{z}_i(t)\}$$

where the equations of the speeds in the directions of motion are:

$$\{\dot{x}_i(t) = \gamma \cdot \dot{x}_i(t-1) + \delta \cdot \ddot{x}_i(t), \ \dot{y}_i(t) = \gamma \cdot \dot{y}_i(t-1) + \delta \cdot \ddot{y}_i(t),$$
$$\dot{z}_i(t) = \gamma \dot{z}_i(t-1) + \delta \cdot \ddot{z}_i(t)\}$$

where the term in the coefficient γ was introduced by Olfati-Saber and Murray [5] and represents a form of elementary memory of the agents (Markov I type relationship in the speed variation equations). The acceleration of the agent i depends on the neighborhood force (3) acting on i, the agent-to-prey force (5) on i, and the friction force (4) of i:

$$\ddot{x}_i(t) = (\gamma - 1) \cdot \dot{x}_i(t-1) +$$
$$+ \sum_{j \in V_i} \vec{F}_{internal}(i,j) \cdot \frac{x_i(t-1) - x_j(t-1)}{d(i,j)} +$$
$$+ \lambda_x \cdot (x_p(t-1) - x_i(t-1)) - \mu \cdot \dot{x}_i(t-1)$$

$$\ddot{y}_i(t) = (\gamma - 1) \cdot \dot{y}_i(t-1) +$$
$$+ \sum_{j \in V_i} \vec{F}_{internal}(i,j) \cdot \frac{y_i(t-1) - y_j(t-1)}{d(i,j)} +$$
$$+ \lambda_y \cdot (y_p(t-1) - y_i(t-1)) - \mu \cdot \dot{y}_i(t-1)$$

$$\ddot{z}_i(t) = (\gamma - 1) \cdot \dot{z}_i(t-1) +$$
$$+ \sum_{j \in V_i} \vec{F}_{internal}(i,j) \cdot \frac{z_i(t-1) - z_j(t-1)}{d(i,j)} +$$
$$+ \lambda_z \cdot (z_p(t-1) - z_i(t-1)) - \mu \cdot \dot{z}_i(t-1)$$

D. Remarks on Movement Equations

We recognize that the equations of motion of the agent i are forced second-order nonlinear differential equations where the forcing term is given by the trajectory of the prey. Since the equations depend on the agent index i, the dynamic of the swarm is that of a coupled system of nonlinear differential equations of the following form:

$$\{\ddot{x}_i + \varphi(\dot{x}_i) + \Psi(x_i, x_j) = \lambda_x \cdot x_{prey}(t)$$
$$\ddot{y}_i + \varphi(\dot{y}_i) + \Psi(y_i, y_j) = \lambda_y \cdot y_{prey}(t) \qquad (6)$$
$$\ddot{z}_i + \varphi(\dot{z}_i) + \Psi(z_i, z_j) = \lambda_z \cdot z_{prey}(t)\}_{1 \leq i,j \leq N}$$

where the coupling is done by the term $\Psi(x_i, x_j)$ (the swarm cohesion forces) and N is the number of agents in the swarm. We take as initial conditions the positions, speeds, and accelerations of all swarm agents at timestep $t = 0$. The average of the accelerations $\ddot{x}_i$, $\ddot{y}_i$, $\ddot{z}_i$ for every timestep t represent the pixels of the three output images. The image-swarm interaction is discussed in detail in the following section. Notice that linearizing the coupled system of differential equations (6) we would obtain a system of coupled linear, damped, oscillators. The local behavior would be similar to that of the model by Elkaim *et al.* [1] in that locally the forces would be elastic.

E. Non-Euclidean Swarm Distance Perception

We introduce a swarm dynamic with non-Euclidean distance function instead of the Euclidean $d(i, j)$ used in the previous sections. While the use of Euclidean distance in literature seems natural for determining agent interactions, this choice is not justified by biological facts. In biological swarming, the distances between individuals are determined through a means of communication that allows swarm members to determine their relative distance, based on a senses, such as odor, hearing, and vision. Recent research on locust swarming showed that odor was mediating neighbor interactions [6]. There is no evidence that odor is producing measurements based on an Euclidean distance. We departed from the biological swarming models, that typically use Euclidean distance by using non-Euclidean distance metrics might be valuable for image enhancement using swarm processing algorithms. As an example, we used a logarithmic distance function and applied the resulting swarm filter to the two input images. The logarithmic distance function we used is:

$$d(i, j) =$$
$$\log\left(1 + \eta \cdot \sqrt{(x_i - x_j)^2 + (y_i - y_j)^2) + (z_i - z_j)^2}\right)$$

where we used values of η ranging from 1 to 10 in increments of 1 per simulation. The output images using the logarithmic distance did not show any improvement over the input images. Nonetheless, we consider the analysis of non-Euclidean distances for the swarm algorithm to be a direction for future work, specifically designing distance functions that enable the emphasis of desired features in the input images.

F. Image Processing Algorithm and Implementation Details

An image is represented by a matrix M indexed over $i, j \in \mathbb{N}$, where (i, j) represent the positions of the pixel (range $0 \leq i \leq x_{max}$, $0 \leq j \leq y_{max}$), and the values in the matrix represent grayscale levels (range 0 to 255). The number of timesteps used in the simulation corresponds to the number of pixels $x_{max} \cdot y_{max}$ in the input image. Each timestep t corresponds to a different pixel in the image, as follows: starting with the first horizontal line in the input image($i = 0$), traverse each line in the input image in order left-to-right $j = 0$ to $j = y_{max} - 1$ and store the graycale value of the current pixel (i, j) corresponding to timestep $t = i \cdot y_{max} + j$ into the prey's x, y, and respectively z coordinate values:

$$\{x_p(t) = \chi_x \cdot M(i, j), \; y_p(t) = \chi_y \cdot M(i, j),$$
$$z_p(t) = \chi_z \cdot M(i, j)\} \qquad (7)$$

where $M(i, j)$ denotes the grayscale value for pixel (i, j). The use of different coefficients χ_x, χ_y, χ_z coefficients in (7) allows the application of three different swarm filters on the same input image. Computing the average of the swarm agents' accelerations at every timestep t for the x, y, and z directions of motion allows the output of three images that are obtained from converting the $\ddot{x}(t)_{avg}$, $\ddot{y}(t)_{avg}$, $\ddot{z}(t)_{avg}$ values of the swarm into grayscale values. If the values are above the grayscale value of 255 they are truncated to 255 in the resulting image (the same holds for negative values which we truncate to a grayscale value of 0). The resulting images varied significantly based on the values of the χ coefficients.

The swarm's positions, speeds, and accelerations are pseudorandomly generated for $t = 0$ as initial conditions. The values of all parameters in the algorithm are fixed at the initialization step. Also in the initialization step all values of x_p, y_p, and z_p are computed and stored. As described in sect. 2.1, the accelerations of a given agent i depend on determining the forces acting upon i from its neighbors $j \in V_i$. The implementation has been done in C.

III. RESULTS

For determining the power and the limits of the swarm image processing, we performed simulations on two abnormal Mammographies from the NIH [18] (see Fig. 1). The area of interest in the input images consists of the calcified deposits. The calciferous deposits produced by cancer are depicted in the input images by an arrow. The problem in mammography imaging is to de-blur the image and to eliminate the useless details for evidencing the micro-calcifications. Typical image enhancement procedures, like contrast manipulation and histogram equalization are only partly effective in this respect, as they emphasize various useless details at the same time with the micro-calcifications (see Fig. 4). In fact, histogram equalizers may further mask the calcification into the details of the scene, as in Fig. 5. In contrast, after the swarm filtering, the elements of interest are shown over a flat, almost uniform gray surrounding. The nonlinear filter emphasizes these Ca

deposits as in Fig. 3. However, the swarm processing results depend on the processed image and may produce results similar to the ones obtained based on histogram manipulation. The case is exemplified in Fig. 1 and Fig. 5.

During the simulations, we adjusted the parameters of the algorithm in order to emphasize the deposits with respect to the surrounding tissue. We produced output images either using the acceleration of the center of mass of the swarm or the speed of the center of mass of the swarm as the filter (see Fig. 3, Fig. 1).
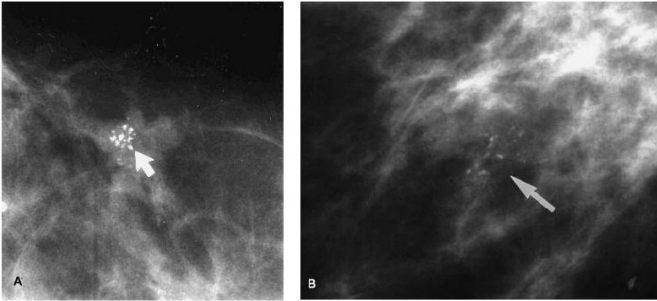
Fig. 1. Input Mammographic Images A and B, adapted from NIH [18], used to demonstrate the nonlinear filter.
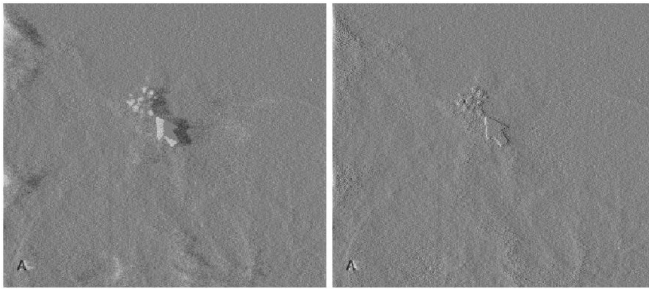

Fig. 2. Feature extraction for input image A using the z-acceleration (left panel) and x-acceleration (right panel) of the center of mass of the swarm as differentiator filters and $\chi_x = 30$, $\chi_z = 10$.
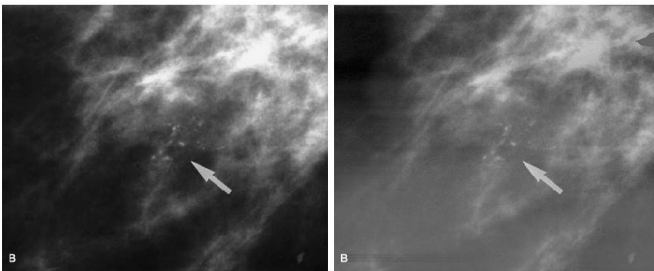

Fig. 3. Original input image B (left panel) versus filtered image using the z-acceleration of the center of mass (right panel) using $\chi_z = 1$.

We performed numerous simulations on the input images to empirically determine ranges of values for the parameters that resulted in usable output images. We varied the swarm
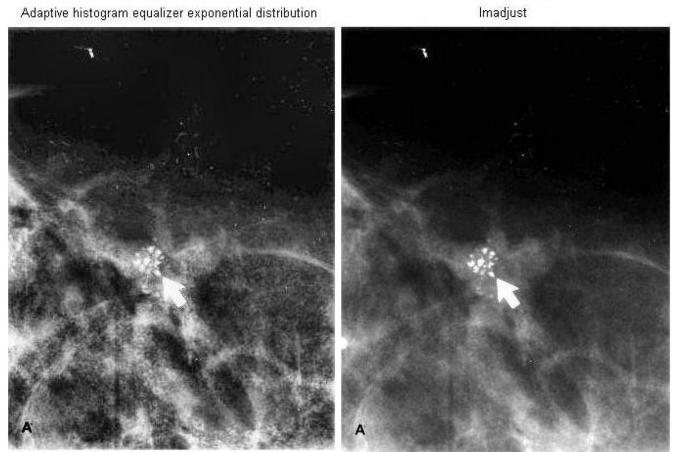

Fig. 4. Results obtained with histogram manipulation on the first mammographic image (left panel) and contrast adjustment (right panel)
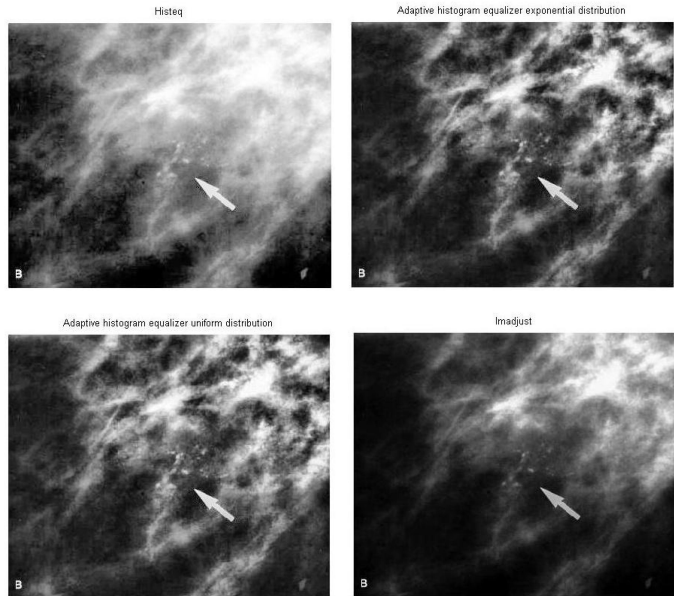

Fig. 5. Results obtained with histogram manipulation on the second mammographic image

size between 5 agents, which we experimentally determined to be the minimum size of swarm that would affect the input image, and 50 agents in increments of 5. Maintaining all other parameters constant, swarms larger than 25 agents had the same effect on the input image as swarms of size 25 agents. The parameter γ had a significant impact on the output image. A value of γ larger than 1 resulted in a uniform gray image (no features), while values of γ under 0.5 in decrements of 0.1 decreased the contrast of the image until no features were visible for γ of 0.1. We obtained the best results regarding emphasizing the features of interest in the image with values of γ between 0.9 and 0.98. The friction coefficient μ also had a significant impact on the result image. We varied μ in

increments of 0.1 from 0 to 1.5. No features were obtained for μ of 0 and for μ above 1. The neighborhood threshold distance ρ variation from 1 to 150 had no significant impact on image quality. The value of δ used in the output images Fig. 2 was of 0.15 and in Fig. 3 was of 0.0005 and the number of agents in the swarm used for both figures was 25. The coefficients λ_x, λ_y, λ_z, α, and β were set at the value of 1 throughout the simulations. A major impact on the output images was due to the χ_x, χ_y, χ_z coefficients, which, when distinct from each other, would generate three distinct output images. An example of this effect is shown in Fig. 2, where the two distinct images were obtained for the same set of parameters and same input image, except for $\chi_x \neq \chi_z$ and resulted in different filtering applied in the swarm's x and respectively z directions of motion. Since the swarm dynamic is highly nonlinear, changing one of the three χ coefficients while keeping the other two constant as in a previous run will change all three output images. The values used to illustrate this difference between the x output image and the z output image in Fig. 2 were $\chi_x = 30$, $\chi_y = 5$, and $\chi_z = 10$. The values of $\chi_x = 30$, $\chi_y = 5$, $\chi_z = 1$ are used in Fig. 3.

IV. CONCLUSIONS

While image processing, including feature emphasis, has recently benefited of many artificial intelligence techniques such as neural networks and genetic algorithms, not to mention various combinations of statistic filters, tasks like mammographic image processing remained unsatisfactory solved. In the research reported here, we devoted ourselves to conceiving a method that could make use of the elementary collective intelligence of the swarms to tackle image processing. We introduced a novel nonlinear swarm dynamic that incorporates non-Euclidean agent distance perception and which we apply to image processing. While we exemplified feature emphasis on MRI mammography images, the method could be extended for feature emphasis in other classes of images and be trained in view of feature recognition.

The interaction forces between the agents and the image relief that we used in this paper may be somewhat unnatural for a biological swarm, hence the research should continue in identifying new types of interaction forces that, on one side, are closer to the natural ones and, on the other side, preserve or enhance the filtering results.

The research presented is incipient. Extensive tests must be performed on a variety of images under a large spectrum of noises to check the robustness of the filters proposed. Also, the quality of the results was not the same for different classes of processed images, each class requiring a trimming of the swarm coefficients to perform well or at least acceptably. Thus, we need to derive an automated optimization procedure of the swarm processing system before the method can see extended use. Future collaboration with experts in the medical field is essential in determining the degree of utility of the swarm signal processing in mammography and in other imaging fields.

REFERENCES

[1] G. H. Elkaim and M. Siegel, "A lightweight control methodology for formation control of vehicle swarms," in *Proc. IFAC 2005*, Prague, July 4-8 2005.
[2] G. H. Elkaim and R. J. Kelbley, "Extension of a lightweight formation control methodology to groups of autonomous vehicles, in *Proc. ISAIRAS 2005*, Munich, September 5-9 2005.
[3] A. Olshevsky and J. N. Tsitsiklis, "Convergence rates in distributed consensus and averaging," in *Proc. IEEE 45th Conference on Decision and Control*, pp. 3387-3392, December 13-15 2006.
[4] R. Olfati-Saber and R.M. Murray, "Consensus problems in networks of agents with switching topology and time-delays," *IEEE Trans. on Automatic Control*, Vol. 49, No. 9, September 2004.
[5] R. Olfati-Saber, J.A. Fax, and R.M. Murray, "Consensus and cooperation in networked multi-agent systems," in *IEEE Proceedings*, Vol. 95, No. 1, pp. 215-233, January 2007.
[6] M. L. Anstey, S.M. Rogers, O. M. Swidbert, M. Burrows, and S.J. Simpson, "Serotonin mediates behavioral gregarization underlying swarm formation in desert locusts," *AAAS Science*, Vol. 323, pages 627–630, January 30 2009.
[7] M. G. Naumann, "Swarming behavior: evidence for communication in social wasps," *AAAS Science*, Vol. 189, pp. 642–644, August 22 1975.
[8] Y.D. Lubin, "Dispersal by swarming in a social spider," *AAAS Science*, Vol. 216, pp. 319–321, April 16 1982.
[9] R. A. Morse "Swarm orientation in honeybees," *AAAS Science*, Vol. 141, pp. 357–358, July 26 1963.
[10] J. H. Todd, J. Atema, and J. E. Bardach, "Chemical communication in social behavior of a fish, the Yellow Bullhead (Ictalurus natalis)," *AAAS Science*, Vol. 158, pp. 672–673, November 3 1967.
[11] A.S. Feng, P.M. Narins, C.-H. Xu, W.-Y. Lin, Q. Qiu, and Z.-M. Xu, "Ultrasonic communication in frogs," *Nature Letters*, Vol. 440, pp. 333–336, March 16 2006.
[12] V.S. Arch, T. U. Grafe, and P.M. Narins, "Ultrasonic signaling by a Bornean frog," *Biology Letters*, Vol. 4, pp. 19–22, February 23 2008.
[13] V. Ramos, F. Muge, and P. Pina, "Self-organized data and image retrieval as a consequence of inter-dynamic synergistic relationships in artificial ant colonies," in *Javier Ruiz-del-Solar, Ajith Abraham and Mario Kppen (Eds.), Frontiers in Artificial Intelligence and Applications, Soft Computing Systems - Design, Management and Applications, 2nd Int. Conf. on Hybrid Intelligent Systems*, IOS Press, Vol. 87, pp. 500–509, Santiago, Chile, December 2002.
[14] V. Ramos and F. Almeida, "Artificial ant colonies in digital image habitats - a mass behavior effect study on pattern recognition," arxiv.org/abs/cs/0412086.
[15] P. Huang, H. Cao, and S. Luo, "An artificial ant colonies approach to medical image segmentation," *Computer Methods and Programs in Biomedicine*, Vol. 92, pages 267–273, Elsevier, 2008.
[16] T. Huang and A.S. Mohan, "A Microparticle Swarm Optimizer for the Reconstruction of Microwave Images," *IEEE Transactions on Antennas and Propagation*, Vol. 55, Issue 3, pp. 568–576, March 2007.
[17] L. Ma, K. Wang, and D. Zhang, "A universal texture segmentation and representation scheme based on ant colony optimization for iris image processing," *Computers and Mathematics with Applications*, Vol. 57, pages 1862–1868, Elsevier, 2009.
[18] J. Holland and E. F. Frei, "Cancer Medicine," *NIH NCBI Bookshelf*, Fifth Edition, Chapter 30, Fig. 30F.12, March 2007.